Earth Syst. Sci. Data Discuss., 7, 305–334, 2014
www.earth-syst-sci-data-discuss.net/7/305/2014/
doi:10.5194/essdd-7-305-2014

Open Access Earth System Science Data Discussions

Lake surface water temperatures of European Alpine lakes (1989–2013) based on the Advanced Very High Resolution Radiometer (AVHRR) 1 km data set

M. Riffler[1,2] **and S. Wunderle**[1,2]

[1]Oeschger Centre for Climate Change Research, University of Bern, Bern, Switzerland
[2]Institute of Geography, University of Bern, Bern, Switzerland

Received: 25 March 2014 – Accepted: 6 April 2014 – Published: 6 May 2014

Correspondence to: M. Riffler (michael.riffler@oeschger.unibe.ch)

Published by Copernicus Publications.

Title Page
Abstract | Instruments
Data Provenance & Structure
Tables | Figures
◀| |▶
◀ ▶
Back | Close
Full Screen / Esc
Printer-friendly Version
Interactive Discussion

Abstract

Lake water temperature (LWT) is an important driver of lake ecosystems and it has been identified as an indicator of climate change. Thus, the Global Climate Observing System (GCOS) lists LWT as an Essential Climate Variable (ECV). Although for some European lakes long in situ time series of LWT do exist, many lakes are not observed or only on a non-regular basis making these observations insufficient for climate monitoring. Satellite data can provide the information needed. However, only few satellite sensors offer the possibility to analyse time series which cover 25 years or more. The Advanced Very High Resolution Radiometer (AVHRR) is among these and has been flown as a heritage instrument for almost 35 years. It will be carried on for at least ten more years finally offering a unique opportunity for satellite-based climate studies. Herein we present a satellite-based lake surface water temperature (LSWT) data set for European (pre-alpine) water bodies based on the extensive AVHRR 1 km data record (1989–2013) of the Remote Sensing Research Group at the University of Bern. It has been compiled out of AVHRR/2 (NOAA-07, -09, -11, -14) and AVHRR/3 (NOAA-16, -17, -18, -19 and Metop-A) data. The high accuracy needed for climate related studies requires careful pre-processing and consideration of the atmospheric state. Especially data from NOAA-16 and prior satellites were prone to noise, e.g., due to transmission errors or fluctuations in the instrument's thermal state. This has resulted in partly corrupted thermal calibration data and may cause errors of up to several Kelvin in the final resulting LSWT. Thus, a multi-stage correction scheme has been applied to the data to minimize these artefacts. The LSWT retrieval is based on a simulation-based scheme making use of the Radiative Transfer for TOVS (RTTOV) Version 10 together with operational analysis and reanalysis data from the European Centre for Medium Range Weather Forecasts. The resulting LSWTs were extensively validated using in situ measurements from lakes with various sizes between 14 and 580 km^2 and the resulting biases and RMSEs were found to be within the range of −0.4–0.6 K and 1.0–1.9 K, respectively. The upper limits of the reported errors could be rather attributed to

Title Page
Abstract | Instruments
Data Provenance & Structure
Tables | Figures
◀| |▶
◀ ▶
Back | Close
Full Screen / Esc
Printer-friendly Version
Interactive Discussion

uncertainties in the data comparison between in situ and satellite observations than inaccuracies of the satellite retrieval. The cross-platform consistency of the retrieval was found to be within ∼ 0.2 K. A comparison with LSWT derived through global sea surface temperature (SST) algorithms shows lower RMSEs and biases for the simulation-based approach. A running project will apply the developed method to retrieve LSWT from the northern part of Finland to southern Italy to derive the climate signal of the last 30 years. The data are available at doi:10.1594/PANGAEA.831007.

1 Introduction

The interest in lake surface water temperature (LSWT) is manifold. The temperature of lakes is an important parameter for lake ecosystems influencing the dynamics of physio-chemical reactions, the concentration of dissolved gazes (e.g. oxygen), and vertical mixing (Delpla et al., 2009). Even small temperature changes may already have irreversible effects on the lacustrine system due to the high specific heat capacity of water. All these effects will finally influence the quality of lake water depending on parameters like lake size and volume (Delpla et al., 2009, and references therein).

Numerous studies (e.g., Adrian et al., 2009; Williamson et al., 2009) mention lake water temperature as an indicator of climate change and within the Global Climate Observing System (GCOS) implementation plan (GCOS-138, 2010), it is stated that "observing the surface temperature of lakes [. . .] can serve as an indicator for regional climate monitoring". Recent studies (e.g., Schneider and Hook, 2010; Lenters et al., 2012) have shown that many lakes are getting warmer more rapidly than the ambient air temperature and more work is needed to be done to explain these differences. This warming trend also affects the onset of freezing and duration of ice cover of many lakes, especially in northern latitudes and mountainous regions (Jensen et al., 2007; Dibike et al., 2011).

Beside the climate and ecological importance of water temperatures, LSWT is also of interest for modelling purposes, since sufficiently large water bodies influence mesoscale weather development and LSWT can be assimilated in regional numerical weather prediction models (Balsamo et al., 2012) to make regional forecasts more precise.

In contrast to in situ observations, satellite imagery offers the possibility do derive spatial patterns of LSWT variability. Moreover, although for some European lakes long in situ time series exist (e.g., Livingstone and Dokulil, 2001; Livingstone, 2003), the temperatures of many lakes are not monitored or only on a non-regular basis making these observations insufficient for climate monitoring. In GCOS-154 (2011) it is further stated that trial products of satellite-based LSWT would be desirable.

The Remote Sensing Research Group at the University of Bern (RSGB), Switzerland, is hosting a large data set from the Advanced Very High Resolution Radiometer (AVHRR), a heritage instrument which has now been flown for almost 35 years on the National Oceanic and Atmospheric Administration (NOAA) Polar Operational Environmental Satellites (POES) and on the Meteorological Operational Satellites (MetOp) from the European Organisation for the Exploitation of Meteorological Satellites (EUMETSAT). It will be carried on for at least ten more years, thus offering a unique opportunity for satellite-based climate studies.

Nowadays, several different satellite-based LSWT data sets are available (e.g., Politi et al., 2012; MacCallum and Merchant, 2012; Schneider and Hook, 2010), but most of them cover only large lakes (with a surface area of $> 500\,\mathrm{km}^2$). Oesch et al. (2005) successfully demonstrated that LSWT can also be retrieved for smaller lakes like the majority of the European alpine water bodies. This data set, however, is only available for a limited time period and more importantly, the technique applied has been developed for the retrieval of sea surface temperatures which may lead to biases in the retrieved temperatures. More modern retrievals (e.g., MacCallum and Merchant, 2012; Hulley et al., 2011) are lake specific taking the lake altitude (i.e. thickness of the atmosphere) and local meteorological conditions into account.

The data set presented herein is based on a regionally optimized technique and covers lakes with sizes of $> 14\,\mathrm{km}^2$ for the period 1989–2013. The Radiative Transfer for TOVS (RTTOVS) and European Centre for Medium Range Weather Forecasts (ECMWF) reanalysis data were used to improve the retrieved LSWT by correcting for atmospheric water vapour effects.

The following section specifies the lake locations and data used to derive the proposed data set. Section 3 explains the LSWT retrieval in more detail. In Sect. 4, we present a comparison of the satellite-based LSWTs and in situ measurements for various sample lakes. The last section summarises the findings and gives a short outlook on future activities.

2 Data

This section lists the European (pre-)alpine lakes included in the proposed data set, the lakes for which in situ data is available to validate the LSWT retrieval, and a detailed description of the satellite data used in order to derive LSWT.

2.1 Lakes

The data set includes all major European alpine lakes (25; cf. Table 1) with sizes from 14 km^2 (Lake Sempach) to 580 km^2 (Lake Geneva). The focus on smaller lakes is an advantage for future climate studies because global satellite-based LSWT data sets (e.g., Schneider and Hook, 2010) include only the two largest (> 500 km^2) of them, whereas 18 out of 25 lakes presented herein have sizes between 14 and 100 km^2 and 5 of them cover areas between 100 and 370 km^2. Artificial water bodies or lakes used for hydro-electric power generation are not included. In addition, Lake Woerth has also been excluded from the data set, since AVHRR is not able to properly resolve this narrow and elongated lake. According to the European Environment Agency (Stanners and Bourdeau, 1995), about 16 000 lakes in Europe are larger then 1 km^2 with $\sim 2000 > 10$ km^2, ~ 150 of them between 100 and 400 km^2 (without man-made reservoirs) and 24 of them covering areas > 400 km^2. With this study we want to demonstrate the potential to derive LSWT for climatological studies from satellite data for the many lakes in Europe within the size range between approximately 15 (depending on the shape) and 500 km^2, which is the limit used in the study of Schneider and Hook (2010). Of course, such a data set can hardly be provided on a global scale (with ~ 12 300 inland waters in the range of 10–100 km^2; Reynolds, 2007), but it offers great potential for regional or even continental scale climate analyses.

2.2 In situ data

The lakes in Switzerland are a representative sample for all alpine lakes in terms of size, shape, and altitude. Therefore, the validation of the retrieval of LSWT was done only for Swiss lakes.

Table 2 lists the lakes and locations with in situ data which were available for the validation of the LSWT retrieval. For the largest lakes (Geneva, Constance) several locations with hourly or daily bulk measurements (0.5–1 m depths) covering most of the period between 1989 and 2013 were usable. The other (smaller) lakes are usually probed vertically once per month, except for Lake Zurich with daily to bi-weekly probes. Although many of these monthly data sets provide observations since the late 80's or early 90's, only few coincident in situ and satellite observations have been found.

2.3 AVHRR

The NOAA and MetOp AVHRR data from NOAA-11, -12, -14, -16, -17, -18, -19, and Metop-A (M02) between 1989 and 2013 at full resolution (1.1 km × 1.1 km at nadir) have been used for this data set. NOAA-15 has not been considered, since the data has been found to be of lower quality than from the other satellites (e.g., Cao et al., 2001; Wu et al., 2009). Metop-B was only launched in September 2012 and has not been considered in the current data set. Figure 1 gives an overview of data availability per satellite and month for this period in the archive of the Remote Sensing Research Group at the University of Bern. The current version of the algorithm contains daytime data only, although in general night time data are found to give slightly better results (e.g., Oesch et al., 2005; Schneider and Hook, 2010; MacCallum and Merchant, 2012), but the additional information from the visible channels during daytime offers advantages for the detection of clouds and discrimination between land and water pixels at small lakes. Up to NOAA-14, the satellites carried the five channel AVHRR/2 sensor (0.6, 0.8, 3.7, 11.0, 12.0 µm), as of NOAA-15, the six channel AVHRR/3 (0.6, 0.8, 1.6, 3.7, 11.0, 12.0 µm) has been flown. For the lake surface water temperature retrieval, channel 4 (T_4; ∼ 11 µm) and channel 5 (T_5; ∼ 12 µm) are used in the split-window equation, whereas the visible ($R_{0.6}$) and near-infra-red ($R_{0.8}$) channels provide additional information for the cloud mask and quality assessment. The pre-processing of the data, including calibration of the visible channels, geocoding, orthorectification, cloud and cloud shadow detection, is described by Hüsler et al. (2011) in more detail. For the retrieval of LSWT, thermal calibration and stability is a key issue and the procedure to convert the data from the raw sensor counts to the final brightness temperature differs from the description in Hüsler et al. (2011). These differences and associated effects will be discussed in the following section.

Thermal calibration

In contrast to AVHRR channels 1 ($R_{0.6}$) and 2 ($R_{0.8}$), which use vicarious calibration (Yu and Wu, 2009) based on stable reflectance targets and inter-satellite comparisons (Heidinger et al., 2010), the thermal channels (3/3B, 4, and 5) offer the possibility of on-board calibration making use of two reference measurements, one against an internal calibration target and the other by measuring into deep space (Goodrum et al., 1999). From this, a high quality output signal would be expected. However, due to errors during the signal transmission and reception, solar contamination during the measuring cycle (at low sun elevation), the sensor signal might be corrupted substantially (e.g., Trishchenko, 2002; Wu et al., 2009). The standard calibration technique of NOAA (Goodrum et al., 1999) does only consider minor fluctuations by averaging the calibration information (sensor signal from measuring into deep space and an internal calibration target, temperature measurement of the internal calibration target) over a few scan cycles. Thus, such corruptions of the signal will partially or fully propagate into the final brightness temperatures and may lead to errors of up to a few Kelvin (Trishchenko, 2002).

Despite the lack of independent information to estimate signal errors, the calibration information (signal from deep space and internal calibration target measurement, as well as the measured temperature of the target) provided during each scan cycle can be analysed for consistency since the nature of the calibration targets should lead to rather stable calibration signals with slow rates of change in time (Trishchenko, 2002). Thus, Trishchenko (2002) proposed a method to better control unwanted fluctuations during the calibration cycle by using a multi-stage filtering technique, which is a combination of robust statistical methods and Fourier transform filtering. More details are given in Trishchenko (2002).

For this data set, we implemented this technique and compared the resulting brightness temperatures for channel 4 (T_4) and 5 (T_5) as well as the effect of this procedure onto the final LSWT retrieval. Figure 2 shows the differences in the resulting channel brightness temperatures for NOAA-16 between 2001 and 2004 by comparing the mean brightness temperatures for a whole satellite scene (from North Cape/Scandinavia to Northern Africa) when using the standard calibration method of NOAA (orig) and the adjusted calibration (filt) after Trishchenko (2002). It becomes obvious that periods with signal corruptions frequently occur and the different calibration techniques lead to temperature differences of several Kelvin, although it has to be admitted that especially NOAA-16 had problems with the scan motor (cf. NOAA Satellite and Information System, Office of Satellite Operations, NOAA-16 AVHRR Subsystem Summary, http://www.oso.noaa.gov/poesstatus/). Most of the AVHRR-carrying satellites used for this data set show intermittent periods with corrupted signal. Figure 3 demonstrates the effect of using either the original NOAA (orig) or the adjusted (filt) calibration methods onto the final LSWT for a sample period in January 2002. The observations highlighted with the orange circle was corrupted and the adjusted method is capable of retaining a reliable signal. The proposed data set has been prepared with the adjusted calibration technique described above.

3 Lake water temperature retrieval

3.1 Split-window approach

Water acts almost as a black body in the thermal infra-red (TIR) region. Assuming that the atmosphere is totally transparent would allow to measure LSWT directly as the water-leaving radiation making use of a single TIR measurement. Atmospheric trace gases (mainly water vapour), however, act as absorbers and emitters and alter the water-leaving radiation leading to a combined atmosphere–surface-signal at sensor level which is why atmospheric correction becomes necessary. Anding and Kauth (1970) found that the differences of two neighbouring TIR channels (e.g., T_4 and T_5) are proportional to the correction needed which is the basis for the so-called "split-window" technique.

Linear and non-linear correction approaches have been proposed in the past (e.g., Walton et al., 1998). Results from several studies (e.g., Li et al., 2001; Oesch et al., 2005) have shown that the linear version of the multi-channel split-window equation gives slightly better results (lower biases) than the non-linear equation of Walton et al. (1998). Thus, we use similar to Hulley et al. (2011) the linear multi-channel equation

$$\mathrm{LSWT} = a + bT_4 + c(T_4 - T_5) + d(T_4 - T_5)[1 - \sec(\Theta_\mathrm{v})], \tag{1}$$

where T_4 and T_5 are the brightness temperatures of AVHRR channel 4 (~ 11 µm) and 5 (~ 12 µm), $\sec(\Theta_\mathrm{v})$ is the secant of the viewing angle Θ_v, and coefficients a to d depict the split-window coefficients.

Deriving coefficients a to d can be done either by applying a fit between in situ and satellite observations or by applying radiative transfer codes with a set of representative LSWTs to create a database of simulated satellite observations and fitting these two parameters. Various studies (e.g., Oesch et al., 2005; Politi et al., 2012) have shown that LSWT over Europe can be derived with reasonable accuracy making use of global split-window approaches designed for sea surface temperature (SST) retrievals by comparing in situ observations of ocean water temperature with satellite data. These methods, however, are intended to match the global atmospheric conditions over ocean surfaces which may substantially differ from the continental conditions found over some inland water bodies. Therefore, other studies (e.g., Hulley et al., 2011; MacCallum and Merchant, 2012) have elaborated more accurate methods to retrieve LSWT by utilising radiative transfer codes and atmospheric data from numerical weather prediction (NWP) re-analyses and analyses data to better reproduce the atmospheric conditions in such regions and also account for the lake specific altitude. In addition, the latter methods have the advantage that they are completely independent of in situ data and therefore also applicable to situations far away from in situ observations, whereas Politi et al. (2012), for instance, use in situ observations to adapt their retrievals for local effects.

In order to derive coefficients a to d of Eq. (1) for the proposed data set, we made use of a simulation-based data set for the European alpine lakes. For this, we used a representative set of LSWTs together with atmospheric profiles (21 pressure levels) of temperature and relative humidity as well as the mean sea level pressure at lake height and 10 m wind speed. These data are available from the European Centre for Medium Range Weather Forecasts (ECMWF) ERA-40 reanalysis (until mid-2002; Uppala et al., 2005) and operational analysis data (from 2002–2013) and were fed into the fast Radiative Transfer for TOVS Version 10 (RTTOV-10; Saunders et al., 2012) to create a database of simulated satellite observations. For the LSWT input into RTTOV-10, we used the NWP 2 m-temperature $T_{2\,\mathrm{m}} \pm 10\,\mathrm{K}$ with increments of 5 K of every cloud-free satellite overpass. This was done for different regions to the north and south of the Alps. In addition, for each overpass we used eight different Θ_vs (from 0 to 60°). Finally, we derived daily split window coefficients by applying a robust multi-linear fit between the simulated satellite data and the LSWT and included ±180 days of simulations for the calculation of the coefficients. We tried shorter and longer time periods, but found the most accurate results (lowest bias) for this time interval. Finally, the retrieved temperatures were adjusted to bulk water temperature making use of the wind-speed-dependent parametrisation of Minnett et al. (2011). Although this correction has been derived from ocean data and may not be appropriate under all circumstances for lakes, it mostly reduces the bias between LSWT and in situ observations in the study region.

3.2 Quality testing

After the retrieval of LSWT, several tests examined on the data ensure that the resulting temperatures are not contaminated with cloudy or land surface pixels. These tests encompass the information generated from the Cloud and surface parameter retrieval (CASPR; Key, 2002), from the cloud shadow mask (Simpson and Stitt, 1998), and additional tests, which have been introduced to enhance the quality of cloud and land detection over (small) inland water bodies. Water surfaces are generally characterised by low reflectance values in the visible ($R_{0.6}$) and near-infra-red ($R_{0.8}$) with $R_{0.8} < R_{0.6}$ caused by higher absorption of radiation for longer wavelength, whereas over land surfaces chlorophyll absorption leads to $R_{0.6} < R_{0.8}$. This information can be used for a simple discrimination of land and water pixels during daytime. A threshold of $R_{0.8} < 0.08$ turned out to be appropriate for the study region and removed most part of non-detected cloud pixels. We applied an additional test to identify mixed (land and water) pixels making use of the ratio between the $R_{0.8}$ and $R_{0.6}$ channel (cf. Schwab et al., 1999). For cloud-free pixels fully covered with water, the $R_{0.8}/R_{0.6}$-ratio is typically less then unity. Schwab et al. (1999) applied a threshold of 0.75 to exclude cloudy pixels. In our study region, this value turned out to be too strict, especially for small water bodies the ratio for cloud-free conditions (visual inspection of the data) was often found to be between 0.75 and 1.0. Therefore, we adjust this threshold to 1.0, although this might cause some misclassification over large lakes. The land-water-mask has been derived from a combination of a Moderate Resolution Imaging Spectroradiometer (MODIS) reference image and the Global Self-consistent, Hierarchical, Highresolution

Shoreline Database (GSHHS; Wessel and Smith, 1996). Pixels not fully covered by water are masked out. The LSWT retrieval is restricted to $-5\,^{\circ}\mathrm{C} \leq \mathrm{LSWT} \leq 35\,^{\circ}\mathrm{C}$, which is a meaningful range for the investigated area and colder surfaces are either cloudy, frozen, or caused by sensor errors (Kilpatrick et al., 2001). The local standard deviation $\sigma_{3\times3}$ is calculated for each pixel, if at least 2 out of 9 pixels are available in the 3×3 pixel matrix. The higher the value of $\sigma_{3\times3}$, the more likely a pixel is contaminated with clouds. Similar to Schneider and Hook (2010), we examine a threshold of $\sigma_{3\times3} \leq 0.5\,\mathrm{K}$ to the data. As highlighted in other studies (e.g., Oesch et al., 2005; Kilpatrick et al., 2001), increasing Θ_v leads to erroneous retrievals due to the increased instant field-of-view (IFOV) causing distortions towards the edges of satellite imagery, increased errors in the split-window equation, and prolonged atmospheric pathway of the lake-leaving radiance (Kilpatrick et al., 2001; Oesch et al., 2005). Therefore, retrievals with $\Theta_\mathrm{v} > 45^{\circ}$ were discarded from the further analysis.

Specular reflection of sun light – sun glint – over water surfaces leads to highly reflecting regions under particular observation and sun geometries. This effect is mostly harmful in the visible and short wave infra-red region, whereas the influence in the spectral range of AVHRR channel 4 (11 µm) and 5 (12 µm) is almost negligible. In rare cases, sun glint might cause a temperature deviation of a few tenth degree Kelvin. We evaluated the effect by comparing in situ observations and satellite-based water temperatures with and without sun glint. Excluding the sun glint area lowers the root mean square error (RMSE) and bias by 0.1–0.2 K, however, the exclusion of these pixels brings along a substantial reduction (> 50 %) in usable LSWTs. For this reason, we decided to keep pixels affected by sun glint.

4 Validation

The proposed data set has been extensively validated with in situ data from various lakes (cf. Table 2) with sizes between 14 and 580 km^2. For the comparison with in situ observations, LSWT has been averaged over 3×3 pixels if at least 2 out of 9 clear-sky pixels were available. At in situ locations with hourly data (cf. Table 2), the two closest in situ observations have been linearly interpolated to match the satellite overpass. For all other in situ sampling rates (daily, weekly, monthly), we compared measurements which have been taken on the same day as the satellite overpass. This can cause a time difference of several hours between both measurements. Possible impacts of this difference will be discussed below.

Applying the optimized split-window approach based on RTTOV-10 (RT-lswt) reduces the bias of the retrieved LSWT compared to a global SST approach (e.g., Oesch et al., 2005). To demonstrate this effect, we also applied the split-window approach presented in Oesch et al. (2005) which is based on the global NOAA NESDIS SST product.

Figure 4 shows a few validation results for various satellites and locations by applying RT-lswt. The upper row presents the comparison between NOAA-17 (AVHRR/3) LSWT-retrievals and hourly in situ measurements from Lake Geneva (left, cf. EPFL in Table 2), Lake Constance at the location of Lake Überlingen (centre, KONS) and the Harbour of Bregenz (right, BDS1). The row in the middle exhibits the results for the same in situ locations, but for the data of NOAA-14 carrying the AVHRR/2 sensor. Overall, these plots demonstrate good agreement between in situ (OBS) and satellite (SAT) temperatures with a coefficient of determination (R^2) of 0.95 or higher. The bias, as the mean differences and standard deviation between OBS and SAT, can be found between 0.2 ± 1.0 K at BDS1 and -0.4 ± 1.4 K at EPFL for NOAA-17, whereas for NOAA-14 slightly higher values between -0.3 ± 1.3 K (EPFL) and 0.6 ± 1.4 K are apparent. Negative biases mean that satellite-derived values are higher than in situ observations. EPFL and BDS1 reflect the retrievals for large lakes, whereas the station KONS is located in a fjord-like part, called Lake Überlingen, of Lake Constance which is merely 2–3 km wide and about 21 km long (~ 60 km^2). This clearly demonstrates the potential of the AVHRR-based retrieval by using the 1 km resolution data set and even for such a narrow water body reasonable and accurate temperature retrievals are possible.

Even smaller lakes or lakes with more complex topographic conditions can be used for LSWT retrieval, due to precise geocoding and orthorectification. This is demonstrated with the results from Lake Sempach (SPS; 14 km^2), Lake Murten (MRS; 23 km^2), or Lake Thun (TNS; 48 km^2). The scatter plots from the lower row highlight the comparison between monthly in situ profiles and satellite-derived temperatures of these three water bodies. As stated in the previous section, due to the low observations frequency, only few coincident data points have been found and, therefore, all satellites are put together into a single figure and the statistics were calculated using all data pairs. Again, values of $R^2 > 0.96$ prove the reasonability of the satellite retrievals, although it has to be admitted that due to the limited number of coincident pairs the robustness of the statistics is limited (higher confidence intervals than for hourly observations). The biases (-0.1 ± 1.5 K to -0.7 ± 1.6 K) are somewhat higher than for larger lakes. We attribute part of the larger error to the fact that for these comparisons the time of the in situ measurement is not exactly known. For these data sets, only the day of observation is available meaning that a time difference of several hours between observation and satellite overpass could be possible. The results from the narrow Lake Überlingen (cf. KONS in Fig. 4) support this assumption, nonetheless, to further estimate the impact of such a time difference, we used the hourly resolved data set at KONS to calculate the spread between daily minimum and maximum temperature at 0.5 m depth. The resulting range can be up to 4 or 5 Kelvin (cf. Fig. 5a), especially during summer months and is mostly driven by the radiation budget and the meteorological conditions (Hook et al., 2003; Minnett et al., 2011). Periods with large amounts of incoming solar radiation and/or calm situations will cause large diurnal temperature variations, whereas cloudy (low incoming solar radiation) or windy days will redistribute the energy more evenly in the uppermost layers leading to a lower spread (Oesch et al., 2005). Therefore, the uncertainty introduced into the validation by using the data without exact observation time is larger than for the hourly resolved data. In addition, the amount of data pairs is biased toward summer observations, because periods with persistent coverage of low level clouds can frequently be found during winter months.

Not only do differences in the observational times introduce uncertainty to the analysis, but also physical reasons behind the measurement techniques. Whereas in situ measurements are often carried out in a depth of 0.5–1.0 m, satellite sensors observe a sub-micron (skin) layer at the water surface. Although we did not have in situ profiles from the water surface (skin layer) to deeper layers available to exactly quantify the resulting difference, some information about the potential impact can be seen from Fig. 5b. The curve depicts the instantaneous temperature differences between 0.5 and 0.9 m depth at KONS for the period 2004–2007, which frequently exceed values of 0.5 K, especially during summer months. The differences are largest for calm and cloud-free situations with high incoming solar radiation. Thus, we applied a skin-to-bulk correction (Minnett et al., 2011), as described in Sect. 3, which lowers the bias between in situ and satellite-based temperature in order to adjust the satellite-based retrieval towards the bulk temperatures.

As mentioned in the description of the satellite data set above, several AVHRRs, flown on various NOAA and MetOp satellites, were necessary to cover the period between 1989 and 2013. As a consequence, the stability of the retrieval (consistency of the resulting data) is of crucial importance. To evaluate the stability of the retrieval with respect to the various satellites in use, Table 3 shows an overview of the validation statistics for the regional adapted retrieval (RT-lswt) for each satellite. In addition, the results for the global approach (based on NOAA NESDIS, NN-lswt; Oesch et al., 2005) are listed as well to enable the comparison between both methods. Although the results for Lake Constance at BDS1 and BDS2 are rather similar, the regional method RT-lswt generally outperforms the global approach NN-lswt indicated by lower biases and RMSEs (this holds also true for all other lakes and locations). The drop of the RMSE from N14 to N16 (and the following satellites) is most likely caused by the change from daily (BDS1) to hourly (BDS2) in situ data. The comparison between NOAA-16 and in situ data at EPFL exhibits RMSEs and biases which are substantially higher than for the other in situ-satellite data pairs. Since the comparison at Lake Constance (BDS1 and BDS2) does not show a similar behaviour, we are convinced that the in situ data at EPFL during that time are not reliable. Considering the EPFL data comparison for NOAA-14, -17, -18, -19, and MetOp-A, for which period time sampling and location of the in situ location have not changed, one can see that across the different satellites the LSWT retrieval is stable within ∼ 0.2 K (RMSE and bias). The same comparison for NN-lswt exhibits a stability within ∼ 0.6 K. One problem with the NOAA NESDIS approach is that the split-window coefficients have not been calculated for all satellites in a consistent manner resulting in uncertainties of the final LSWTs.

Calculating the total bias over all satellites results in 0.4 ± 1.2 (RT-lswt) and -0.2 ± 1.3 (NN-lswt) for Lake Constance (BDS1/2), respectively, and -0.5 ± 1.5 (RT-lswt) and -0.9 ± 1.7 (NN-lswt) for Lake Geneva (EPFL), respectively. The bias of all satellites combined at Lake Zurich is 0.1 ± 1.2 (RT-lswt) and -0.8 ± 1.7 (NN-lswt), respectively. At Lake Neuchatel we get 0.1 ± 1.2 (RT-lswt) and -0.3 ± 1.3 (NN-lswt), respectively. NN-lswt generally exhibits slopes of the regression equation around 1.1 meaning that especially during summer months temperature is overestimated with the NOAA NESDIS coefficients in use, whereas for RT-lswt the slope is close to unity.

One exception in the performance of RT-lswt is NOAA-12 with a significant higher RMSE and bias for the regional methods with systematically too cold water temperatures derived from the satellite data. NOAA-12 overpasses were typically during the morning causing the satellite-observed skin layer to be cooler than deeper layers, i.e. bulk temperature (Hook et al., 2003). Since we apply a skin-to-bulk-correction (Minnett et al., 2011) in the regional model approach to better reflect temperatures from subsurface layers this might even introduce a larger bias, because the correction always leads to an adjustment toward cooler temperatures.

5 Summary and conclusions

The radiative transfer-based LSWT retrieval presented herein is a state-of-the-art method to derive lake water temperature from AVHRR sensor data independently of in situ measurements. Similar to other studies, we have shown that with such an approach more accurate retrievals of LSWT than with a method designed for global SST retrieval are possible. Initially, the pre-processing of AVHRR data is an important step and, although the thermal channels of AVHRR feature on-board thermal calibration, special treatment of the sensor signal is needed to guarantee a good quality of observed brightness temperatures. The validation against in situ observations exhibits biases in the range of −0.4–0.6 K and RMSEs of 1.0–1.9 K, even though the upper limit of reported errors may rather be attributed to uncertainties in the spatio-temporal match-up between satellite and in situ data than to inaccuracies of the retrieved LSWTs. Results for small ($> 14\,\text{km}^2$) and medium sized lakes are similar to large lakes like Lake Constance and Lake Geneva which also highlights the need for precise geocoding and orthorectification of AVHRR data. In order to avoid misclassification at the interface between land and water for small lakes, the data set is currently confined to daytime observations only, since daytime data allows to use the visible and short-wave infra-red channels to discriminate land from water pixels as well as mixed pixels. The consistency across the different satellites is stable within $\sim 0.2\,\text{K}$. For instance, the increase of lake temperature of the last 30 years retrieved from in situ measurements is in the range of $0.054\,^{\circ}\text{C}\,\text{yr}^{-1}$ for Lake Zurich (Adrian et al., 2009). Therefore, the accuracy of the presented method to retrieve LSWT is sufficient for climate related studies to detect a significant warming trend.

The intercomparison with in situ data demonstrated that AVHRR data not only provide spatially consistent information on LSWT, but also enable the extension of in situ time series back in time. Therefore, this data set can be seen as an important contribution to climate observations; e.g. many lakes in Switzerland are only monitored on an irregular basis.

The current version of the data set is available for all major European (pre-)alpine lakes with sizes between 14 and $580\,\text{km}^2$ for the time from 1989 to 2013. Further improvements to the data set will be the expansion back in time (early 1980ies) and spatially to the main water bodies in entire Europe since AVHRR is the only sensor offering such long time series. The influence of volcanic aerosols to the retrieval will also be evaluated and we also plan to include the night time data as well.

Supplementary material related to this article is available online at http://www.earth-syst-sci-data-discuss.net/7/305/2014/essdd-7-305-2014-supplement.zip.

Acknowledgements. This project has been funded by the Swiss GCOS Office, Federal Office of Meteorology and Climatology, MeteoSwiss. In addition, we are grateful to the NOAA STAR/NESDIS team for providing the operational NOAA SST coefficients. We would also like to thank the Remote Sensing Group from the Rosenstiel School of Marine and Atmospheric Science for providing Pathfinder SST coefficients. Without the many providers of in situ observations, this work would not have been possible. Thus, we would like to thank Frank Peeters from the U. Constance, Claude Perrinjaquet from EPF Lausanne, Ralf Grabher from Abteilung Wasserwirtschaft – Land Vorarlberg, several cantonal agencies in Switzerland, and the Institut National de la Recherche Agronomique (INRA).

References

Adrian, R., O’Reilly, C. M., Zagarese, H., Baines, S. B., Hessen, D. O., Keller, W., Livingstone, D. M., Sommaruga, R., Straile, D., Van Donk, E., Weyhenmeyer, G. A., and Winder, M.: Lakes as sentinels of climate change, Limnol. Oceanogr., 54, 2283–2297, 2009. 307, 321

Anding, D. and Kauth, R.: Estimation of sea surface temperature from space, Remote Sens. Environ., 1, 217–220, 1970. 313

Balsamo, G., Salgado, R., Dutra, E., Boussetta, S., Stockdale, T., and Potes, M.: On the contribution of lakes in predicting near-surface temperature in a global weather forecasting model, Tellus A, 64, 15829, doi:10.3402/tellusa.v64i0.15829, 2012. 308

Bavarian Lakes, Bayerisches Landesamt für Umwelt: available at: http://www.lfu.bayern.de/wasser/seen_in_bayern/index.htm, last access: 20 March 2014. 327

Beiwl, C. and Mühlemann, H.: Atlas der natürlichen Seen Österreichs mit einer Fläche ≥ 50 ha, Tech. rep., Bundesamt für Wasserwirtschaft, Institut für Gewässerökologie, Fischereibiologie und Seenkunde, Wien, Österreich, 2008. 327

Swiss Lakes, Bundesamt für Statistik: available at: http://www.bfs.admin.ch/bfs/portal/de/index/themen/02/22/lexi.Document.20703.xls, last access: 20 March 2014. 327

Cao, C., Weinreb, M., and Sullivan, J.: Solar contamination effects on the infrared channels of the advanced very high resolution radiometer (AVHRR), J. Geophys. Res., 106, 33463–33469, doi:10.1029/2001JD001051, 2001. 310

Delpla, I., Jung, A.-V., Baures, E., Clement, M., and Thomas, O.: Impacts of climate change on surface water quality in relation to drinking water production, Environ. Int., 35, 1225–1233, 2009. 307

Dibike, Y., Prowse, T., Saloranta, T., and Ahmed, R.: Response of Northern Hemisphere lake-ice cover and lake-water thermal structure patterns to a changing climate, Hydrol. Process., 25, 2942–2953, doi:10.1002/hyp.8068, 2011. 307

Dokulil, M. T.: European Alpine Lakes, Blackwell Science Ltd, 159–178, doi:10.1002/9780470750506.ch6, 2007. 327

GCOS-138: Implementation Plan for the Global Observing System for Climate in Support of the UNFCCC (2010 Update), vol. GCOS-138 of GCOS (Series), World Meteorological Organization, available at: http://books.google.ch/books?id=3WkrNAAACAAJ, 2010. 307

GCOS-154: Systematic Observation Requirements for Satellite-based Products for Climate–2011 Update, Supplemental details to the satellite-based component of the “Implementation Plan for the Global Observing System for Climate in Support of the UNFCCC (2010 Update)”, vol. GCOS-154 of GCOS (Series), World Meteorological Organization, 2011. 308

Goodrum, G., Kidwell, K. B., Winston, W., and Aleman, R.: NOAA KLM user’s guide, US Dept. of Commerce, National Oceanic and Atmospheric Administration, National Environmental Satellite, Data, and Information Service, National Climatic Data Center, Climate Services Division, Washington DC, 1999. 311, 332

Heidinger, A. K., Straka, W. C., Molling, C. C., Sullivan, J. T., and Wu, X.: Deriving an inter-sensor consistent calibration for the AVHRR solar reflectance data record, Int. J. Remote Sens., 31, 6493–6517, 2010. 311

Hook, S. J., Prata, F. J., Alley, R. E., Abtahi, A., Richards, R. C., Schladow, S. G., and Pálmarsson, S. Ó.: Retrieval of lake bulk and skin temperatures using Along-Track Scanning Radiometer (ATSR-2) data: a case study using Lake Tahoe, California, J. Atmos. Ocean.

Tech., 20, 534–548, doi:10.1175/1520-0426(2003)20<534:ROLBAS>2.0.CO;2, 2003. 318, 320

Hulley, G. C., Hook, S. J., and Schneider, P.: Optimized split-window coefficients for deriving surface temperatures from inland water bodies, Remote Sens. Environ., 115, 3758–3769, 2011. 308, 313, 314

Hüsler, F., Fontana, F., Neuhaus, C., Riffler, M., Musial, J., and Wunderle, S.: AVHRR archive and processing facility at the University of Bern: a comprehensive 1-km satellite data set for climate change studies, EARSeL eProceedings, 10, 83–101, 2011. 311

Jensen, O. P., Benson, B. J., Magnuson, J. J., Card, V. M., Futter, M. N., Soranno, P. A., and Stewart, K. M.: Spatial analysis of ice phenology trends across the Laurentian Great Lakes region during a recent warming period, Limnol. Oceanogr., 52, 2013–2026, 2007. 307

Key, J. R.: The Cloud and Surface Parameter Retrieval (CASPR) system for polar AVHRR, Version 4.0:user's guide, NOAA/NESDIS/ORA, Madison, WI, 2002. 315

Kilpatrick, K. A., Podest, G. P., and Evans, R.: Overview of the NOAA/NASA advanced very high resolution radiometer pathfinder algorithm for sea surface temperature and associated matchup database, J. Geophys. Res., 106, 9179–9197, doi:10.1029/1999JC000065, 2001. 316

Lenters, J. D., Hook, S. J., and McIntyre, P. B.: Workshop examines warming of lakes worldwide, Eos T. Am. Geophys. Un., 93, p. 427, doi:10.1029/2012EO430004, 2012. 307

Li, X., Pichel, W., Clemente-Colón, P., Krasnopolsky, V., and Sapper, J.: Validation of coastal sea and lake surface temperature measurements derived from NOAA/AVHRR data, Int. J. Remote Sens., 22, 1285–1303, 2001. 313

Livingstone, D. M.: Impact of secular climate change on the thermal structure of a large temperate Central European lake, Climatic Change, 57, 205–225, 2003. 308

Livingstone, D. M. and Dokulil, M. T.: Eighty years of spatially coherent Austrian lake surface temperatures and their relationship to regional air temperature and the North Atlantic oscillation, Limnol. Oceanogr., 46, 1220–1227, 2001. 308

MacCallum, S. N. and Merchant, C. J.: Surface water temperature observations of large lakes by optimal estimation, Can. J. Remote Sens., 38, 25–45, 2012. 308, 311, 314

Minnett, P. J., Smith, M., and Ward, B.: Measurements of the oceanic thermal skin effect, Deep-Sea Res. Pt. II, 58, 861–868, 2011. 315, 318, 319, 320

Oesch, D. C., Jaquet, J.-M., Hauser, A., and Wunderle, S.: Lake surface water temperature retrieval using advanced very high resolution radiometer and Moderate Resolution Imaging Spectroradiometer data: validation and feasibility study, J. Geophys. Res., 110, C12014, doi:10.1029/2004JC002857, 2005. 308, 311, 313, 314, 316, 317, 318, 319, 329

Politi, E., Cutler, M. E., and Rowan, J. S.: Using the {NOAA} Advanced Very High Resolution Radiometer to characterise temporal and spatial trends in water temperature of large European lakes, Remote Sens. Environ., 126, 1–11, 2012. 308, 314

Reynolds, C. S.: Lakes, Limnology and Limnetic Ecology: Towards a New Synthesis, Blackwell Science Ltd, doi:10.1002/9780470999271.ch1, 1–7, 2007. 310

Saunders, R., Hocking, J., Rayer, P., Matricardi, M., Geer, A., Bormann, N., Brunel, P., Karbou, F., and Aires, F.: RTTOV-10 Science and Validation Report, Tech. rep., NWP SAF, EUMETSAT, 2012. 314

Schneider, P. and Hook, S. J.: Space observations of inland water bodies show rapid surface warming since 1985, Geophys. Res. Lett., 37, L22405, doi:10.1029/2010GL045059, 2010. 307, 308, 309, 310, 311, 316

Schwab, D. J., Leshkevich, G. A., and Muhr, G. C.: Automated mapping of surface water temperature in the Great Lakes, J. Great Lakes Res., 25, 468–481, 1999. 315

Simpson, J. and Stitt, J.: A procedure for the detection and removal of cloud shadow from AVHRR data over land, IEEE T. Geosci. Remote, 36, 880–897, 1998. 315

Stanners, D. and Bourdeau, P. (Eds.): Europe's environment – the Dobris assessment, European Environment Agency, Luxemburg, 712 pp., 1995. 309

Trishchenko, A. P.: Removing unwanted fluctuations in the AVHRR thermal calibration data using robust techniques, J. Atmos. Ocean. Tech., 19, 1939–1954, doi:10.1175/1520-0426(2002)019<1939:RUFITA>2.0.CO;2, 2002. 311, 312, 331, 332

Uppala, S. M., Kållberg, P. W., Simmons, A. J., Andrae, U., Bechtold, V. Da Costa, Fiorino, M., Gibson, J. K., Haseler, J., Hernandez, A., Kelly, G. A., Li, X., Onogi, K., Saarinen, S., Sokka, N., Allan, R. P., Andersson, E. and Arpe, K., Balmaseda, M. A., Beljaars, A. C. M., Berg, L. Van De, Bidlot, J., Bormann, N., Caires, S., Chevallier, F., Dethof, A., Dragosavac, M., Fisher, M., Fuentes, M., Hagemann, S., Hólm, E., Hoskins, B. J., Isaksen, L., Janssen, P. A. E. M., Jenne, R., Mcnally, A. P., Mahfouf, J.-F., Morcrette, J.-J., Rayner, N. A., Saunders, R. W., Simon, P., Sterl, A., Trenberth, K. E., Untch, A., Vasiljevic, D., Viterbo, P., and Woollen, J.: The ERA-40 re-analysis, Q. J. Roy. Meteor. Soc., 131, 2961–3012, doi:10.1256/qj.04.176, 2005. 314

Walton, C. C., Pichel, W. G., Sapper, J. F., and May, D. A.: The development and operational application of nonlinear algorithms for the measurement of sea surface temperatures with the NOAA polar-orbiting environmental satellites, J. Geophys. Res., 103, 27999–28012, doi:10.1029/98JC02370, 1998. 313

Wessel, P. and Smith, W. H. F.: A global, self-consistent, hierarchical, high-resolution shoreline database, J. Geophys. Res., 101, 8741–8743, doi:10.1029/96JB00104, 1996. 316

Williamson, C. E., Saros, J. E., Vincent, W. F., and Smol, J. P.: Lakes and reservoirs as sentinels, integrators, and regulators of climate change, Limnol. Oceanogr., 54, 2273–2282, 2009. 307

Wu, A., Xiong, X., and Cao, C.: Tracking the calibration stability and consistency of the 3.7, 11.0 and 12.0 µm channels of the NOAA-KLM AVHRR with MODIS, Int. J. Remote Sens., 30, 5901–5917, doi:10.1080/01431160902787703, 2009. 310, 311

Yu, F. and Wu, X.: Removal of contaminated pixels from the desert target for AVHRR vicarious calibration, J. Atmos. Ocean. Tech., 26, 1354–1366, doi:10.1175/2009JTECHA1171.1, 2009. 311

Table 1. List of European (pre-)alpine lakes included in the data set showing their area, volume, and altitude according to Dokulil (2007); Bavarian Lakes, LfU Bayern (2014); Beiwl and Mühlemann (2008); Swiss Lakes, BFS (2014). The geographic co-ordinates indicate the centre location of a 3 × 3 pixel area for which the satellite data has been extracted in order to create the proposed LSWT data set.

Lake name	Lake area [km^2]	Volume [$\times 10^6$ m^2]	Altitude [m a.s.l.]	Latitude	Longitude
Lake Geneva	582	88 900	372	46°24′52″ N	06°24′57″ E
Lake Constance	535	48 400	395	47°36′35″ N	09°25′38″ E
Lake Garda	370	49 000	65	45°32′19″ N	10°38′33″ E
Lake Neuchatel	215	14 170	429	46°57′18″ N	06°56′05″ E
Lake Maggiore	213	37 700	194	45°53′51″ N	08°33′54″ E
Lake Como	146	22 500	198	46°00′50″ N	09°15′45″ E
Lake Lucerne	114	12 280	434	47°01′07″ N	08°22′20″ E
Lake Zurich	88	3767	407	47°13′15″ N	08°43′33″ E
Lake Chiem	80	2048	518	47°53′07″ N	12°28′08″ E
Lake Iseo	62	7600	186	45°44′13″ N	10°04′21″ E
Lake Starnberg	56	2999	584	47°53′47″ N	11°18′26″ E
Lake Lugano	49	6500	271	45°59′29″ N	08°58′10″ E
Lake Ammer	47	1750	533	47°59′01″ N	11°07′41″ E
Lake Thun	48	6500	558	46°41′45″ N	07°42′32″ E
Lake Atter	46	3945	469	47°53′31″ N	13°32′55″ E
Lake Bourget	45	3600	232	45°44′26″ N	05°51′54″ E
Lake Biel	39	1240	429	47°05′01″ N	07°10′28″ E
Lake Zug	38	3200	413	47°09′24″ N	08°29′04″ E
Lake Brienz	30	5200	564	46°44′32″ N	08°00′05″ E
Lake Annecy	27	1120	447	45°51′43″ N	06°10′07″ E
Lake Traun	24	2303	422	47°53′00″ N	13°47′34″ E
Lake Walen	24	2420	419	47°07′15″ N	09°13′47″ E
Lake Murten	23	600	429	46°55′51″ N	07°04′51″ E
Lake Sempach	14	624	504	47°08′34″ N	08°09′18″ E
Lake Mond	14	510	481	47°49′31″ N	13°22′44″ E

Table 2. Summary of lakes and locations with in in situ observations of water temperatures used for the validation of the satellite retrieval. The two values for the size of Lake Constance indicate the area of the entire lake and the area of the subsection of Lake Überlingen. Abbreviations for the various locations are used to easily identify the chosen data set.

Lake	Lake size [km^2]	Location	Position	Time period	Sampling rate	Depth	Abbreviation
Geneva	580	46.46° N, 6.40° E	100 m offshore	2000–2011	hourly	1 m	EPFL
		46.37° N, 6.45° E	shoreline	1991–2011	$T_{\min}$, $T_{\max}$	1 m	INRA
Constance	535 (60)	47.76° N, 9.13° E, Lake Überlingen	1 km offshore	1987–2001	hourly	0.5 m	KONS
				2004–2007	hourly	0.5 m	KONS
		47.51° N, 9.75° E, Harbour of Bregenz	shoreline	1989–1996	daily mean	0.5 m	BDS1
				1997–2009	hourly	0.5 m	BDS2
Neuenburg	215	46.90° N, 6.84° E	mid-lake	2001–2012	monthly	surface	NBS
Zurich	88	47.30° N, 8.57° E	mid-lake	1989–2008	1–2 weeks	surface	ZUE1
		47.35° N, 8.53° E	shoreline	2008–2012	daily	0.5 m	ZUE2
Thun	48	46.68° N, 7.73° E	mid-lake	1994–2012	monthly	surface	TNS
Murten	23	46.93° N, 7.09° E	mid-lake	1989–2011	monthly	surface	MRS
Sempach	14	47.14° N, 8.15° E	mid-lake	1989–2010	monthly	surface	SPS

Table 3. Statistical parameters for all satellites at Lake Constance (BDS1 and BDS2) and Lake Geneva (EPFL) by using the regional LSWT-retrieval based on RTTOV-10 (RT-lswt) and NOAA NESDIS (NN-lswt; Oesch et al., 2005). Shown are the slope (k) and intercept (d) of the linear regression $y = kx + d$ between in situ observation (OBS) and satellite retrieval (LSWT), the coefficient of determination as square of the correlation coefficient (R^2), the root-mean-square error (RMSE), the Bias as the mean temperature difference and standard deviation $\overline{\Delta T} \pm \sigma_{\Delta T}$ between OBS and LSWT, and the number of coincident observations. The comparison for NOAA-11 and -12 at EPFL is missing due to the lack of in situ data for that time.

Sat	RTTOV-10			NOAA NESDIS			N
	R^2	RMSE	Bias	R^2	RMSE	Bias	
Lake Constance, BDS1 and BDS2							
N11	0.95	1.3	0.1 ± 1.2	0.95	1.4	−0.2 ± 1.4	178
N12	0.95	1.9	1.4 ± 1.3	0.96	1.3	−0.1 ± 1.3	74
N14	0.96	1.5	0.6 ± 1.4	0.96	1.6	−0.7 ± 1.5	166
N16	0.98	1.2	0.1 ± 1.2	0.97	1.3	−0.0 ± 1.3	252
N17	0.98	1.0	0.3 ± 0.9	0.98	1.0	0.0 ± 1.0	393
N18	0.98	1.0	0.4 ± 0.9	0.98	1.1	−0.2 ± 1.1	210
N19	0.98	0.9	0.3 ± 0.7	0.98	0.9	−0.0 ± 0.9	44
M02	0.97	1.1	0.5 ± 1.0	0.96	1.2	0.2 ± 1.2	150
Lake Geneva, EPFL							
N11		–			–		–
N12		–			–		–
N14	0.96	1.3	−0.3 ± 1.3	0.95	2.2	−1.6 ± 1.5	106
N16	0.93	2.0	−0.8 ± 1.9	0.93	2.3	−1.0 ± 2.0	371
N17	0.95	1.5	−0.4 ± 1.4	0.94	1.7	−0.7 ± 1.6	608
N18	0.95	1.5	−0.4 ± 1.5	0.95	1.9	−0.9 ± 1.6	418
N19	0.96	1.4	−0.6 ± 1.3	0.95	1.9	−1.2 ± 1.5	134
M02	0.95	1.4	−0.5 ± 1.3	0.95	1.6	−0.7 ± 1.4	293

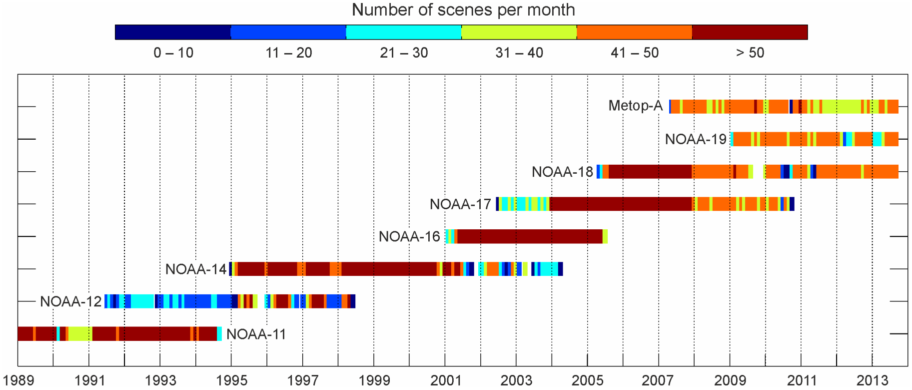

Fig. 1. Number of available satellite overpasses per satellite and month for the period between 1989 and 2013. Shown are all NOAA satellites from NOAA-11 to NOAA-19 and Metop-A. Due to quality issues, NOAA-15 data has been excluded. Metop-B data is also not included in the current version of the data set, since it has only been launched in September 2012. Further data (as of 1984 and for entire Europe) is available in the archive of the Remote Sensing Research Group at the University of Bern, which is currently prepared in an ongoing project.

Title Page
Abstract
Instruments
Data Provenance & Structure
Tables
Figures
◀❙
❙▶
◀
▶
Back
Close
Full Screen / Esc
Printer-friendly Version
Interactive Discussion

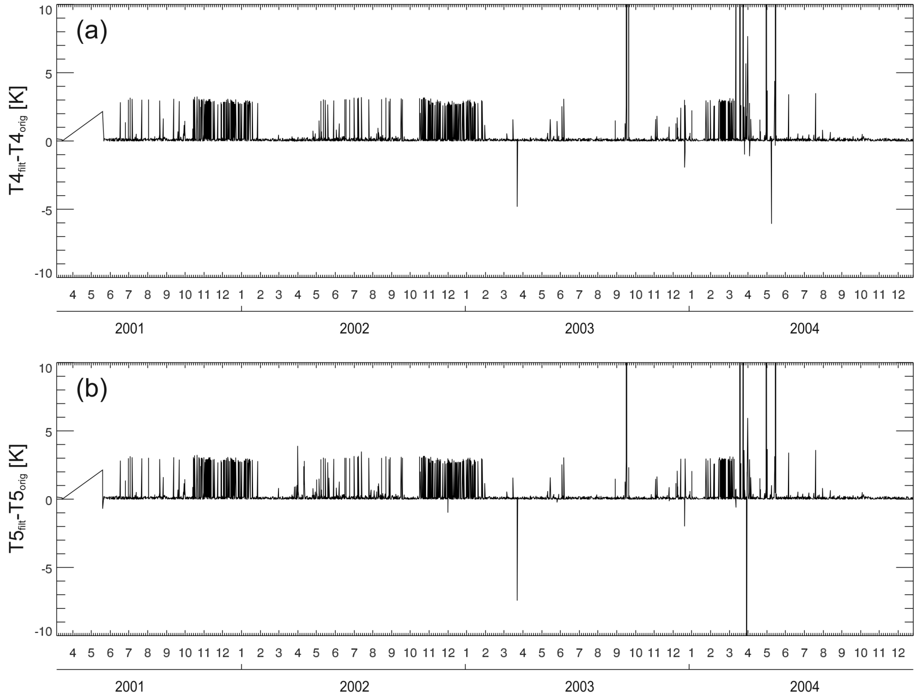

Fig. 2. Mean difference of the scene average brightness temperatures for AVHRR channel 4 **(a)** and 5 **(b)** for NOAA-16 between 2001 and 2004 by using the original NOAA (orig) and adjusted (filt) calibration according to Trishchenko (2002).

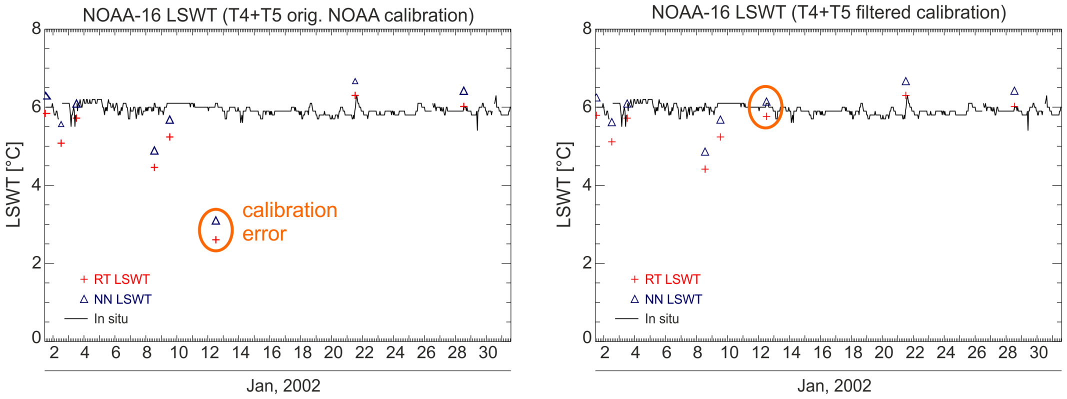

Fig. 3. Comparison of lake temperatures measured in situ (solid line) and retrieved from satellite (symbols) by employing the original (left, Goodrum et al., 1999) and adjusted (right, Trishchenko, 2002) calibration methods to NOAA-16 AVHRR data in January 2002. Encircled in orange is a case for which the sensor signal has been corrupted during the on-board calibration procedure.

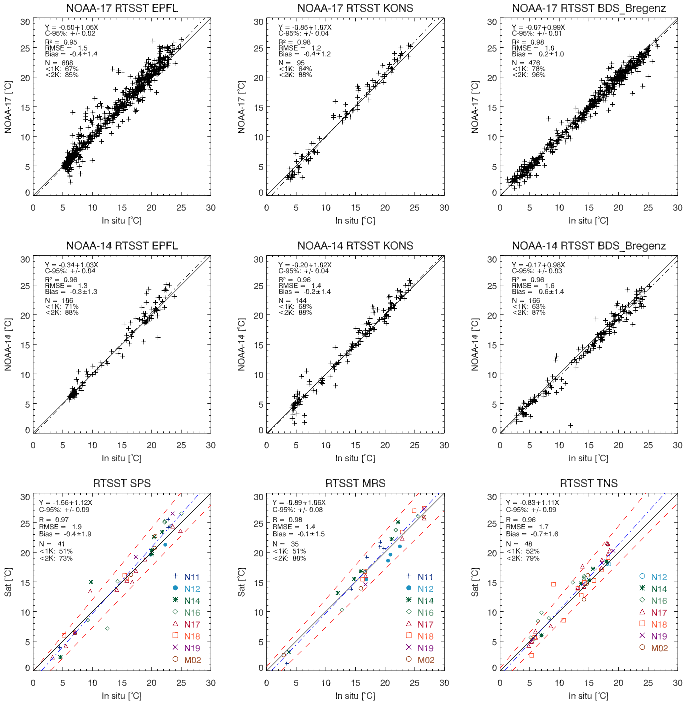

Fig. 4. Scatter plots with the validation between in situ observations (OBS) and the regional LSWT-retrieval based on RTTOV-10 (RT-lswt). Shown are the linear regression equation (dash-dotted), the 95 % confidence interval of the regression line, the coefficient of determination as square of the correlation coefficient (R^2), the root-mean-square error (RMSE), the Bias as the mean temperature difference and standard deviation ($\overline{\Delta T} \pm \sigma_{\Delta T}$) between OBS and RT-lswt, the percentage of values for |RT-lswt – OBS| ≤ 1 K and |RT-lswt – OBS| ≤ 2 K, respectively, and the number of coincident observations. In situ locations are indicated in the graph titles and are explained in Table 2.

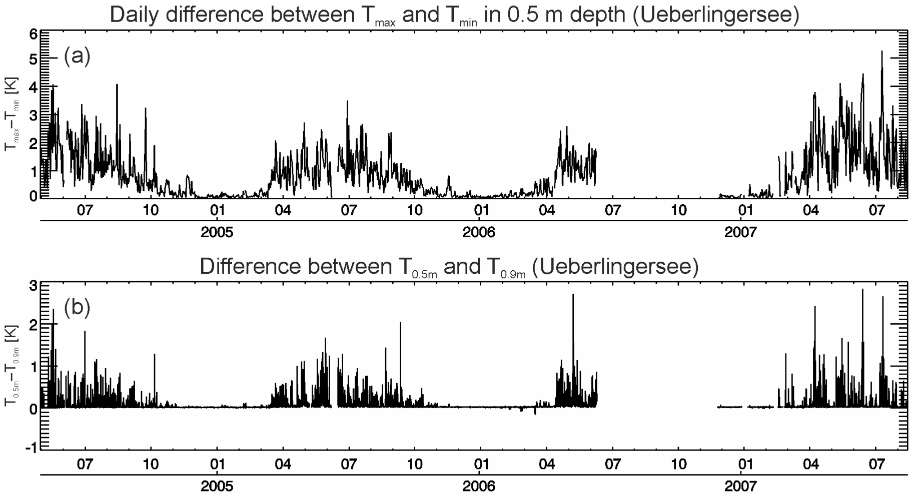

Fig. 5. (a) Daily temperature spread ($T_{max} - T_{min}$) at 0.5 m water depth at Lake Überlingen and **(b)** hourly temperature differences between 0.5 and 0.9 m water depth.